24

Nanoparticles On A String – Fiber Probes as "Invisible" Positioners for Nanostructures

Phillip Olk
NTNU Trondheim
Norway

1. Introduction

Optical fibers have a long and successful history in telecommunications (Howes & Morgan, 1980) and had an enormous global impact on technology and cultural interaction, far beyond just taking telegraphy further (Stephenson, 1996). Aside from transporting data from A to B, optical fibers allowed the exploration of a whole field in photonics research, from fiber-based sensors (Udd, 1990) via various photonic crystal fibers (Zolla et al., 2005) up to quantum optical experiments (Philbin et al., 2008) - current research is presented in this book.
In this chapter, optical fibers are used just as a pointed probe which is basically transparent for light. So most of the originally engineered waveguide properties are ignored, such as low dispersion and absorption for long range applications. Contrary, using optical fibers as scanning probe tips exploits optical and mechanical effects on the nano-scale, i.e., of very close proximity, even less than 5 nm. This is a well-established "abuse" of telecommunication fibers in the Scanning Nearfield Optical Microscope[1], an opto-mechanical tool that is of high benefit in the field of nano-optics (Dunn, 1999). These scanning probe optical microscopes exploit one property of optical fibers that is often overlooked, as it's taken as granted: optical fibers are *transparent*.

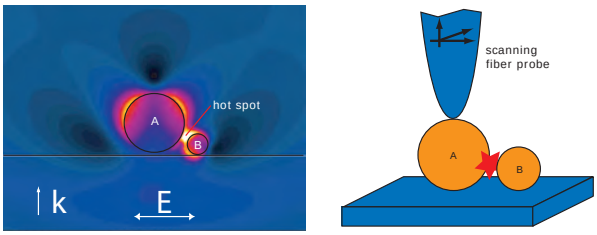

Fig. 1. *Left.* Numerical calculations of the intensity in the vicinity of two metal spheres A and B (Au, 80 nm and 30 nm in diameter, respectively), exposed to a plane wave (λ =532 nm in vacuum). The hot spot has a 20x relative intensity w/respect to the incident wave. *Right.* Suggested experimental implementation: particle A is glued to a 3D-positionable (potentially rotatable) fiber probe, whereas particle B is resting on the substrate.

[1] Abbreviated SNOM, or NSOM, depending on Your current position on the globe.

In the field of nano-optics, the effects of near-fields are applied in order to manipulate light on a scale distinctively smaller than the wavelength of that light. One handy effect is the so-called near-field enhancement at metal structures: a tiny metal rod , i.e. less than $\lambda/4$ in length and only a few dozens of nm in diameter, or a metal sphere can serve as dipole antenna when exposed to a propagating electromagnetic field. The electrons just follow the external electrical field which is oscillating with the frequency of light, and if metal geometry, light frequency and electron mobility/velocity are well trimmed, the particle may exhibit a plasma resonance. If one examines the electric field in the very vicinity of the dipole one will encounter local intensities which are higher than the incident field. In other words: a nanometer-scaled lump of metal may serve as an *optical antenna* and provides enhanced local intensities. As the volume of enhanced intensity is rather small, such a construction can be used as a highly localized light source. E.g., this is applied in tip-enhanced Raman spectroscopy (TERS), where "intensity concentration" is crucial in order to increase the Raman response, which tends to have a very small cross section, but scales with I^2.
Fig.1 depicts a basic application idea of such a nanoantenna: as calculations hint, Fig.1 *left*, a local field enhancement may exist between two nanoparticles, which in turn might be used for experiments such as fluorescence excitation, Raman scattering and similar. In Fig.1 *right*, a sketch is given for a real experimental implementation of such a bi-particle nano-antenna. One particle is attached to a scanning probe, while the second is resting on a substrate. As the actual local field enhancement is highly dependent on the inter-particle distance and the relative orientation to the polarisation, the scanning fiber tip is used as a manipulator in order to optimise the system. Note that no optical properties of the tip are used.
The following sections will provide a detailed insight into the methods of mounting a such single metal nanoparticle to a scanning probe. The reader might keep in mind that the concepts here are not restricted to optical antennas on fiber tips, but can be transferred to different materials for both probe (glass, Si, metals...) and nanoparticle (metal, luminescent nanodiamonds, micelles, cells, molecules etc.), and thus into other wavelength regimes (Wenzel et al., 2008). For the sake of simplicity, only metal nanoparticles are discussed here in detail.
While the idea of, e.g., particle-enhanced Raman spectroscopy is older than the expression "optical antenna" (Wessel, 1985), it turned out to be rather difficult to determine an appropriate nano-particle and subsequently attach it to a scanning probe fulfilling these conditions:

- Exactly the pre-selected particle shall be attached, not just some random item.
- Only this single one shall be attached, not "two, maybe three".
- The particle (especially its optical properties) shouldn't be altered by the pick up process.
- The position and orientation of the attached particle on the probe tip must be known exactly afterwards.

A scientist who is only limited by "technical feasibility" might think of manufacturing techniques such as electron beam lithography: evaporate metal on a glass needle, cut away the surplus metal, done. This certainly is a valid approach, but not everybody has, wants, likes to use, or can afford such an e-beam tool. The technique, as largely introduced by (Kalkbrenner et al., 2001) and continued here, is relatively cheap: if one can afford a SNOM and a usual optical microscope, particle-decorated tips are well within reach.
Most certainly, alternative experiments can generate very similar information about the system of interest. For example, distance-dependent spectroscopy of particle pairs can be realized by producing vast arrays of particle pairs by some lithography technique (Rechberger

et al., 2003), or by pushing single particles into positions by means of a scanning probe (Bek et al., 2008). These techniques are well suitable for two-dimensional positioning, but an experimentalist may encounter a situation where she or he wants to have full control of both position and orientation of a three-dimensional particle in a three-dimensional space – this can be achieved by moving and rotating the particle-decorated scanning probe (Kalkbrenner et al., 2004). As the fiber, especially if immersed in index matching fluid, is hardly visible, the comparison to marionette string puppets is self-evident.

2. Manufacturing particle-decorated fiber tips

This section describes a workflow for attaching a particle to a scanning probe tip for further experiments. Starting from common basics, a few details were optimised, but the procedure may need adaptation for given instruments and circumstances.

2.1 The basic probe design

As a start, an "empty" scanning fiber probe is needed. Depending on time, budget and capabilities, one may either buy a ready-made one or build it from scratch using a raw optical fiber, a quartz tuning fork, and glue. This fiber tip is part of a scanning probe system. Depending on the actual setup and experiment, various mechanisms and realisations are imaginable, Fig. 2, and most of them were successfully applied for particle decoration experiments (Kalkbrenner et al., 2001; Olk et al., 2007; Uhlig et al., 2007). For mid-IR and THz applications, even silicon is more or less transparent, so the SNOM tip may be replaced by a slightly modified AFM cantilever (Wenzel et al., 2008).

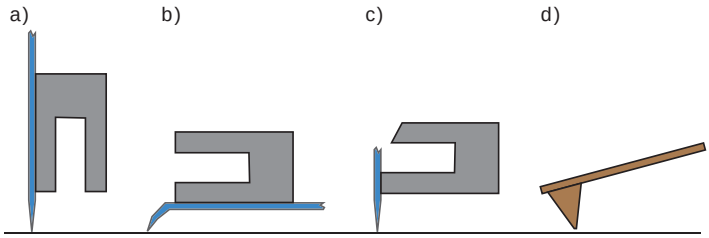

Fig. 2. Variations of scanning probe realizations. a)-c) are based on fiber tips, glued to common quartz tuning forks. d) is a usual AFM tip (Si), which may be sufficiently transparent for IR and THz experiments.

Independent on how the scanning probe is obtained, it is actually desired to have a probe tip *not* as pointed as possible: the tip should not be smaller than the particle that is to be picked. This "trick" allows much bigger tolerances when aligning and positioning the scanning probe with respect to the nanoparticle, Fig.3. In addition, this facilitates the manufacturing process of the pointed fiber itself, as it is not mandatory to use HF acid in order to etch the glass: a heat-and-pull technique, as used in micropipette pullers, can be sufficient.

2.2 Particle decoration

This section provides an all-optical method to pre-select, attach, and check the successful attachment of a desired particle. Depending on the actual experiment, some steps can be

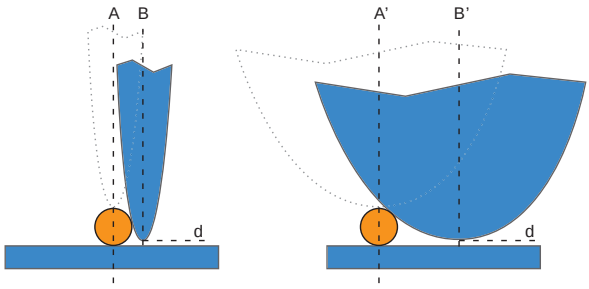

Fig. 3. Tolerances when picking a given particle with a pointed (left) or blunt tip (right). The ideal tip position is hinted by the dotted outlines, and is symmetric to the line A or A', respectively. For a given acceptable minimum vertical tip-sample-distance d, the lateral tolerance is small for pointed tips, $\overline{AB}$, and significantly bigger for blunt tips, $\overline{A'B'}$.

omitted (e.g., the orientation check for spherical particles) or might need to be added (e.g. time-correlated photon counting to check the number of emitters in a nanocrystal).

2.2.1 Particle preparation

Nanoparticles are usually provided as powder, or as suspension in a liquid. For the latter case, a single droplet is applied onto a glass cover slide, as common in microscopy. Depending on the particle density in the suspension liquid, this droplet may just dry (for very low densities), or be sent across the substrate for tens of seconds by a hand-operated rubber blower. As a result, single nanoparticle "candidates" should be distributed over the slide with a next-neighbour-distance big enough so a) single particles can be analysed optically and b) the more or less blunt fiber tip will pick up only one particle.

2.2.2 Optical microscopy of single nanoparticles – the role of homogeneous immersion

For standard microscopy, the Rayleigh criterion is still a valid limit for the resolution. Nonetheless, standard optics are capable to "see" nanoscopic particles:
According to Mie's theory of scattering and absorption of light (plane wave, wavelength λ) at a small (radius $R < \lambda$) conductive sphere, the scattering cross section is proportional to $C_{\text{scat}} \propto R^6$, or, as volume $V = 4/3\pi R^3$:

$$C_{\text{scat}} \propto V^2 \,. \tag{1}$$

So even a very small particle is visible in the eyepiece of a microscope. It can't be *resolved* if close to an other one, but it will produce an Airy disk according to the point spread function of the microscope.[2]
For absorption, Mie provides a similar expression C_{abs}, but this is just proportional to the particle volume:

$$C_{\text{abs}} \propto V \,. \tag{2}$$

In a sketch of these two expressions, Fig.4 *left*, one realises that there exists a crossover size $V_\times$ for the particle, when the lucid scatterer ($C_{\text{scat}} > C_{\text{abs}}$ for $V > V_\times$) turns into an absorber ($V < V_\times$). For a real microscope situation as in Fig.5, this means that the observer faces a

[2] One can still tell single particles from doublets by both intensity and scattering spectrum, as will be explained later.

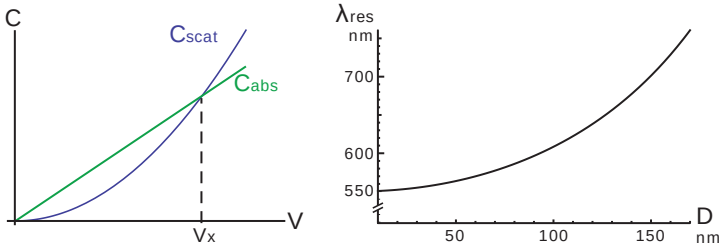

Fig. 4. Optical properties of conductive spheres. *Left*. Qualitative sketch of Mie’s scattering cross section $C_{\mathrm{scat}} \propto V^2$ and absorption cross section $C_{\mathrm{abs}} \propto V$. They cross over at $V_{\times}$. *Right*. Spectral position λ_{res} of the plasma resonance of a particle of diameter D. The numerical values are valid for Au spheres, embedded in an effective medium of refraction $n = 1.52$, and a diameter range from 20 to 160 nm. λ_{res} is a vacuum wavelength, as measured by a (non-immersed) spectrometer.

contrast problem if the particle size is too small: big particles look bright, but in a transient size region, the residual reflection from the cover slide is about as bright as the scattering from the particle – "optical cloaking" without any cape involved. If the particle is even smaller, and the residual reflection is not too intense, the particles may be visible again, but this time, they are dark-on-bright ("bright" being the residual reflection), Fig.5b).

This situation is tightened for "modern standard" microscopy: immersion lenses easily provide numerical apertures NA > 1. This means that larger portions of the illumination light are reflected totally, as the maximum angle of incidence, φ_{NA} is easily bigger than the critical angel of incidence φ_{crit}, Fig.5b). As a result, the background intensity I_{bg} is elevated, so even a lucid scatterer is "swallowed" in contrast to the intense reflection. The solution to this is the homogeneous immersion, Fig.5c): by suppressing any reflection, only the scattering is observed. The idea is rather old (Abbe, 1873), but this is an example of lack of interdisciplinary exchange: scanning probe people prefer a dry environment for their probes, as this facilitates everything (Q factors, controlling etc.). On the other hand, life scientists, who deal with large NA objective lenses since many decades, never were aware of this problem, as they generally *always* use immersion fluids (mostly water).

Depending on the actual nanoparticle, other techniques might be applied in order to locate and identify single particles: absorption-mediated interference microscopy successfully imaged particles smaller than 2 nm (Boyer et al., 2002), and luminescent particles, such as fluorescent PS spheres or N-V centres in nanodiamonds, provide straight forward access to their location. Alternatively, if one succeeds in (self-)arranging nanoparticles in some fixed grid, only relative positioning of the sample is necessary.

A slightly different train of thoughts is valid for the scanning probe tip, which may be considered as a dielectric sphere. Here, absorption is not as important, but the index of refraction: the closer the indexes of the glass tip and the immersion medium are, the less light is "disturbed". Consequently, the tip can’t be located by the bare eye. Indeed, the fiber core itself provides a variation of the index of refraction, an essential property for guiding optical modes, but this is too small to give a significant visual hint on the whereabouts of the fiber.

If there was no immersion medium on the cover slide, the nanoparticle is hardly seen, if the immersion medium matches the slide and the fiber probe too well, the probe vanishes optically. As the experimentalist needs to see both probe tip and particle during the picking

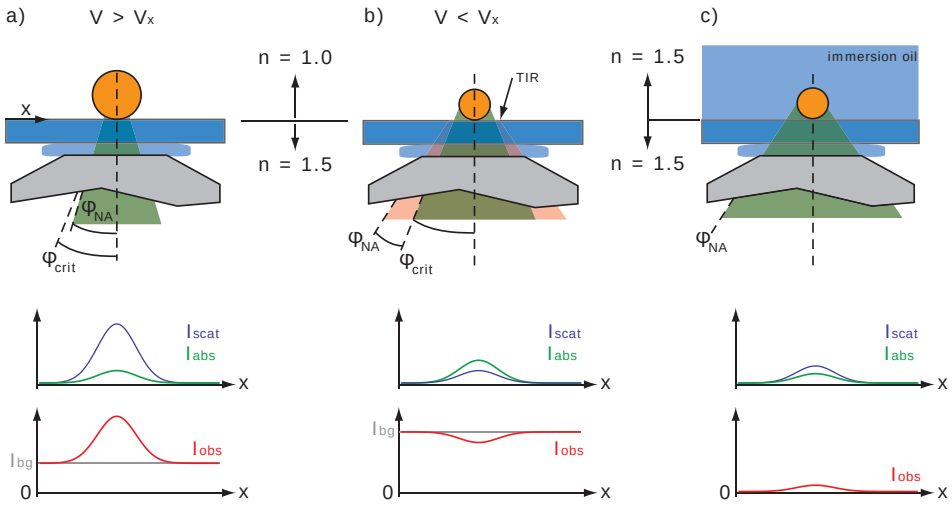

Fig. 5. Illumination schemes (top row) and scattered, absorbed, background and observable intensities for different configurations. a) A sphere of volume $V > V_\times$ scatters more than it absorbs, hence $I_{\text{obs}} = I_{\text{scat}} - I_{\text{abs}} + I_{\text{bg}}$ shows a positive bump – the contrast of the particle is bright on dark. b) For particle volumes $V < V_\times$ the bump is negative, as scattering dominates (dark on bright). In addition, a lens with a larger NA is applied, which increases the background I_{bg} due to total internal reflection (TIR): the red sectors of the incident light are fully reflected. c) Immersion oil on the cover slide removes the refractive index jump and hence any reflection: $I_{\text{bg}} = 0$. The ratio V/λ becomes nV/λ, so the effective wavelength in the medium is smaller. This, in turn, pushes the position of $V_\times$ towards smaller particle volumes.

procedure, a compromise is needed. Instead of a regular immersion oil, which matches common BK7 cover slides and optical fibers too well, a liquid of a lower refractive index is desired. Glycol[3] and glycerin[4] turned out to be suitable, as they are non-volatile, viscous, not too toxic, their index of refraction can be tuned down by mixing with water, and they are easily obtainable. Keep in mind that the immersion liquid between cover slide and microscope lens, i.e. *under* the slide, must be chosen according to the lens manufacturer's specifications.

2.2.3 How to select the right nanoparticle

Selecting an appropriate nanoparticle *before* it is attached to the probe tip is important, as this is the key ability of the procedure provided here. In the case of metal nanoparticles, Mie's theory helps: a single gold sphere, will back-scatter a characteristic spectrum. The peak position λ_0 is related to the diameter D, e.g., a gold sphere embedded in a liquid of a refraction index $n = 1.5$ has its peak position at

$$\lambda_0(D) = \frac{1.15 \cdot 10^9}{2.09 * 10^6 - 20D^2} \,. \tag{3}$$

[3] Ethylene glycol, [107-21-1], $n = 1.43$
[4] Glycerol, [56-81-5], $n = 1.473$

This rule of thumb, derived from (Sönnichsen, 2001), is valid for sphere diameters between 20 and 160 nm, and a powerful handle for size control (Härtling et al., 2008). A plot can be seen in Fig.4 *right*. If the particle of interest was not symmetric, its "effective diameter" would change for different orientations – the peak position is affected according to rotating either the particle or the incident polarisation (Kalkbrenner et al., 2004). As a benefit of this behaviour, the orientation of metal nanowires/ellipsoids/optical antennas can be determined (Olk et al., 2010). In addition, single nanoparticles and multiplets, despite of they can’t be resolved, will produce an Airy disk of a red-shifted colour. For a well-known, reproducible species of nanoparticles, the step of spectral analysis may be omitted, as according to equation 1 an intensity analysis might be sufficient in order to identify "healthy", single nanoparticles.
For nanoparticles differing from metal scatterers, alternative identification methods must be provided, according to the actual requirements of the intended experiment.

2.2.4 Choice of glue

The adhesive needs to provide these properties:

- The nanoparticle must be fastened securely and reliably.
- The glue shouldn’t alter the mechanics of the scanning probe.
- The optical properties of the glue must not interfere with the actual experiment.

For affixing metal nanoparticles to glass, APTMS[5], APTES, or PEI[6] are fine, but other material combinations may demand other specific glues - large plastic spheres can actually be pronged. Detailed procedure descriptions exist in order to obtain densely packed monolayers of these materials. In this application here, such a perfect monolayer isn’t mandatory: it is sufficient to dip the probe tip into a 5-10% aqueous solution of APTMS for some tens of seconds. This allows the silane ends of the molecules to bind to the glass surface. Unbound, excess molecules can be rinsed off by a spill of purified water. As a result, a holey monolayer of amino groups is ready to bind to gold or silver.
The last requirement for the glue, being optically neutral, can turn out to be tricky. For larger particles, a patchy monolayer of molecules isn’t affecting the effective medium strongly. But in a single-molecule Raman spectroscopy experiment, the Raman signal from the glue must not outshine the response from the molecule of interest.

2.2.5 Alignment and attaching

The previous sections provide a scanning probe and a candidate particle. Both tip and particle are very small, so their images are (Airy) disks, probably of different size, colour, and intensity. When setting up a regular scanning probe, the tip is positioned manually some microns over the sample surface. Now the experimentalist aligns the two image disks, frequently jumping forth and back between the two focal planes. A scaled fine drive screw for the microscope will be helpful, as the focal plane of a high-NA lens is very thin. When aligning, two (Airy) disks are centred on each other - the Rayleigh criterion plays no role here. In addition, using a "blunt" tip adds lateral tolerance, as in Fig. 1. In total, the centring tolerance is in the range of the tip radius, which in turn can be close to the (irrelevant) Rayleigh criterion.
Once tip and particle are aligned on the vertical axis, and separated vertically by just one or two micrometers, the actual picking can take place. For most setups, a regular approach procedure at moderate oscillation amplitudes is sufficient: once the tip is "parked" on the

[5] 3-Aminopropyl-trimethoxysilane, [13822-56-5]
[6] Polyethylenemin, [29320-38-5]

nanoparticle for a few seconds, the tip may be retracted. If everything went well, the tip *and the nanoparticle* disappeared from the focal plane - moving the microscope up will bring both back. Moving the tip laterally will quick-check if the particle is actually affixed thoroughly enough. Fig.6 is the corresponding view through the eyepiece of a microscope.

(a) (b) (c)

Fig. 6. Black-and-white optical images of particle-decorated fiber probes. The fiber ($n \approx 1.5$) is immersed in glycol ($n = 1.42$). *Left* The tip produces a V-shaped "shadow" to an external lamp pointing to the upper left of the image. The bright concentric rings (cones actually) stem from fiber-transmitted laser light that is coupled into the other end of the fiber. The white spot in the middle is the back-scattered light from a gold sphere of 80 nm diameter. The illumination scheme corresponds to Fig.5c). *Middle* The laser is switched off, the pointing direction of the external lamp is different now. *Right* The external lamp is switched off, the microscope's illumination is the only remaining light source. The excellent contrast demonstrates the concept of immersed fibers.

To illustrate the possible results, Fig.7 provides some electron microscopy images of particle-decorated tips. Note that an electron image is not necessary for day-to-day quality control, as the procedure, as given here, provides a rigorous check whether the particle is attached or not.

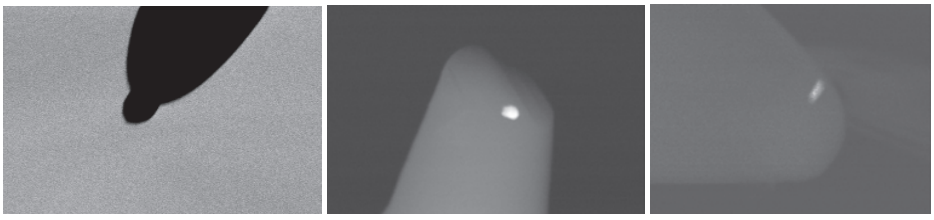

(a) (b) (c)

Fig. 7. SEM images of various particle-decorated tips. a) a 100 nm Au sphere, carbon coated for improved scanning electron imaging. b) Material contrast image of a 80 nm Au sphere. Despite of the broken glass tip, the decoration process worked and produced a usable particle probe. c) Material contrast image of a Ag nanorod, 125 nm in length and 55 nm in diameter. Note the odd spatial orientation of the nanorod.

If the particle refuses to follow the tip, the binding process couldn't take place for several reasons. The nature of these reasons is somewhat unclear, but pressure, time, density of the glue molecules and oscillation amplitude may play a role. Therefore, increasing the normal force by tuning the setpoint may help, as might a reduction of the oscillation amplitude. If this

didn’t lead to success yet, harsher methods may be appropriate: a deliberate disturbance of the distance controller may lead to the desired result. An audible clearing of the throat, coughing, clapping, and, as the last resort, tapping on the optical table (just a soft finger tip), can induce a gentle, but non-ignorable disturbance. Be aware that due to the small area of a nanoparticle, the forces on it may reach easily the magnitude of GPa, which in turn deforms the spherical particle to a heavily patted lump. While this opens the opportunity of nano-minting[7], the change of the shape leads to a visible(!) redshift of the plasma resonance.

2.2.6 Optical antennas - multiple particles

For optical antenna applications, e.g., using a metal nanostructure as a concentrator of the incident field in order to produce a high intensity, say, for Raman scattering experiments, multiple particles turn out to be advantageous, (Fleischer et al., 2008; Jiang et al., 2003; Li et al., 2003; Nie & Emory, 1997; Olk et al., 2007). For this reason, it may seem attractive to obtain particle decorated probes consisting of two (or even more) particles.
Alternatively, one may try to attach the second particle *directly* to the first one, using a specific glue for this purpose: in this case, Au is to be attached to Au, so alkane dithiols (Brust et al., 1995) or more rigid linking molecules (Pramod & Thomas, 2008) are appropriate, if a fume hood is available. A rather flexible link can be achieved by dipping the tip (which is already the first nanoparticle) for 10 minutes into undiluted decanethiol[8]. The residual thiol can be rinsed off by isopropanol. Especially if the second particle is of similar or bigger size than the first one it is recommended to passivate the residual, but unused molecule on the glass tip: for APTMS, exposure to a mild organic acid, mixed into the immersion liquid, turned out to be beneficial. In a straightforward attempt, one may repeat the procedure above and

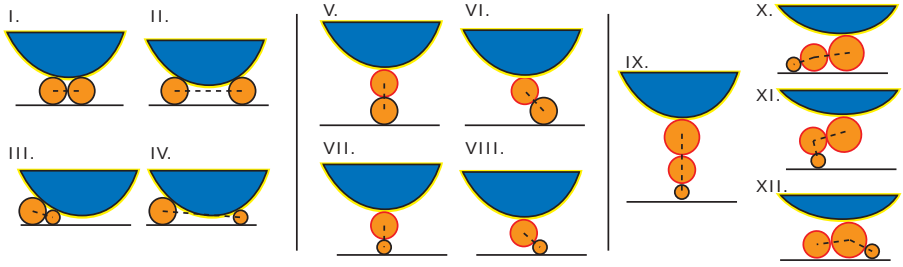

Fig. 8. Possible alignments (only two-dimensional, for the sake of simplicity) for two particles on a tip. The dotted lines connect the particle centres and depict the principal axes. *I.-IV.* If both particles are attached directly to the glass tip. *V.-VIII.* The first particle is affixed to the glass tip by a specific glue (yellow coating), while the second particle is mounted on the first one by a different, specific glue (red coating). *IX.-XII.* Illustration of some mentionable situations for three-particle chains. For small and many particles, quality control by electron microscopy is advised.

affix an additional particle to the glass tip. This will produce particle-decorations as in Fig.8 *left*. Note that in this configuration, the final orientation of the principal axis[9] is dependent on

[7] For comparison: a typical AFM cantilever, spring constant 40 N/m, bent by 50 nm, applies a force of 2 μN. This force, distributed over the projection of a sphere of 25 nm radius, exceeds 1 GPa, more than the yield strength of many metals.
[8] 1,10-Decanedithiol, [1191-67-9].
[9] The line connecting the two centres of the particles.

the particle size, on the distance between the particles, and even on the order of attaching the particles[10]. Generally, the principle axis will be rather horizontal than vertical.
In terms of accuracy, the concepts of Fig.3 can be transferred to this two-particle system, but note that now, the relative position, and consequently, the orientation of the principal axis, is of fundamental importance for the optical antenna effects, Fig.8 *middle*.
The situation "worsens" for particle chains of three or more particles, Fig.8 *right*. If a straight, vertical chain is desired, one has to mind the ways of how the manufacturing process could go wrong. Of course, such "faulty" assemblies may open opportunities for other usage: a folded chain might be considered as a collection of two-particle antennas, each sensitive for a different polarization orientation and/or wavelength.

2.3 Applied scanning particle probes

Two well-established application fields are Scanning Particle-enhanced *Raman Spectroscopy*, and the examination of plasmons on metal nanostructures, e.g. for fluorescence enhancement by means of *optical antennas*, and shall be discussed in detail.
Of course, the concept of a "particle on a string" is not limited to plasmonics and metal particles alone. The reader be reminded of N-V centres in nanodiamonds (Balasubramanian et al., 2008), or quantum dots Aigouy et al. (2006). Future experiments may use single nanowire lasers as a photon source (Johnson et al., 2001), or magnetic nanoparticles as a sensor (Härtling et al., 2010), not to mention antibodies or functional enzymes – the possibilities are virtually endless.

Plasmonics - optical antennas

One important field where the plasmonic properties of metal nanostructures on a tip are exploited, is the field of *plasmonics*. This denotes the discipline of engineering and manipulating metal structures and their optical properties.
An obvious field of research is the examination of the interplay among several metal nanostructures. Thanks to near-field optical coupling, the spectral properties of the metal nanoparticle on the tip is manipulated just by bringing it near to other metal structures - and vice versa. The observed effects vary from plasmon resonance de-tuning (Kalkbrenner et al., 2001; Olk et al., 2008) to four-wave-mixing (Danckwerts & Novotny, 2007).
For single particles, the enhanced near-fields are their most important property. Increasing the local intensity on a restricted volume allows for the *selective* excitation of single fluorescent molecules (Bharadwadj et al., 2007; Frey et al., 2004; Sandoghdar & Mlynek, 1999).

Raman spectroscopy

All progress in the field of enhanced near-field probes quickly found its way into the Raman spectroscopy, probably the most established application of particle-decorated tips. Due to the very small cross sections in Raman scattering experiments, the Raman community depends on high local fields, generated by Surface-Enhanced Raman Spectroscopy (SERS) and Tip-Enhanced Raman spectroscopy (TERS), using massive but pointed wire tips. The concept of optical antennas for local field enhancement was quickly embraced by the community, combined with SERS and TERS concepts, and quickly driven towards near-field enhancing metal nanostructures (Nie & Emory, 1997; Plieth et al., 1999; Stöckle et al., 2000).
The concept of using just one metal particle as an optical antenna, similar to the proposal

[10] Attaching a larger particle first and well on the symmetry axis of the tip will prevent a second, smaller particle from touching the glass tip.

of (Wessel, 1985), was realised early (Anderson, 2000), and has evolved towards RNA sequencing (Bailo & Deckert, 2008). Note that for scanning particle-enhanced Raman microscopy, mostly AFM-based tips with a "thin" metal film (i.e. sputtered metal coagulated to islands, which we consider as nanoparticles here) are used. Aside from the simple fact that attaching a pre-selected particle, as demonstrated here, came later into being (Olk et al., 2007), each experimentalist needs to consider the advantages and disadvantages of the two approaches: price, availability of tools, reproducibility, expected and desired local enhancement, and experimental skills play roles.

3. Demonstration - Fluorescence in the vicinity of two particles

In order to put the concepts of section 2 to a test, two different two-particle systems are analysed by means of fluorescence spectroscopy:
Fig.9 *left* illustrates the basic setup (Olk, 2008): collimated excitation light, controlled in both intensity and polarisation, is focused on the particle system, which is immersed in glycerine dyed with Nile Blue[11]. The linear polarisation of the laser source can either be rotated by a $\lambda/2$ plate or converted to so-called radially polarised light, which produces a focal polarization in the direction of z (Olk et al., 2010). Any fluorescence collected by the focusing lens is guided to a spectrometer. A typical spectrum of pure Nile Blue is in Fig.9 *right*. In a first step, the

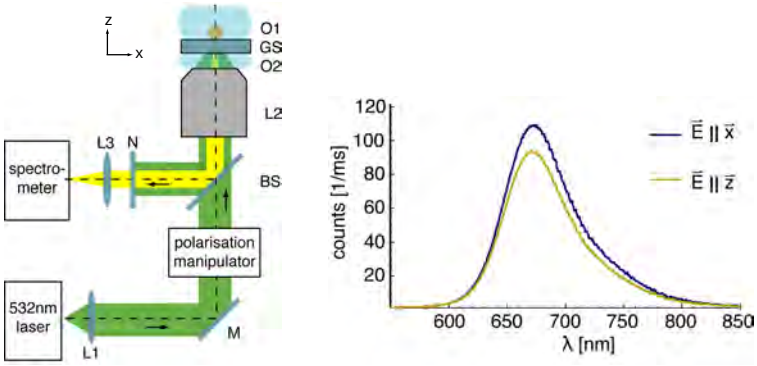

Fig. 9. *Left*. Experimental setup. L2 is a microscope lens requiring immersion oil O2 and a specific glass slip GS in order to perform optimal. O1 is the immersion medium dyed with Nile Blue. *Right*. Typical fluorescence spectra of Nile Blue for two given focal polarizations.

focal plane is moved 30 μm into the Nile Blue glycol, so the focal volume is fully in material that can fluoresce. Then, a fiber tip carrying one single Au particle of 80 nm diameter is inserted into the focus, and the fluorescence intensities are recorded for radially and linearly polarised light, Fig.10 *left*. In comparison to Fig.9 *right*, the fluorescence signal is reduced, approximately by a factor of two. This is owed to the fact that the fiber tip itself displaces the dye, so a good part of the focal volume consists of non-fluorescent glass. This is an effect that is hardly quantifiable, as the indexes of refraction are close. Usually, this is a desired advantage, but here, the similarity of the indices lets the tip vanish for the human eye. This renders it impossible to position the *bare* tip in the focus in order to quantify its displacement.

[11] [3625-57-8]

A different issue that can be learned from Fig.10 *left* is that for a focal z polarisation, the detected fluorescence intensity is much lower than for horizontally polarised excitation light. This can be explained by the inset in that figure: the region of high nearfields at the particle consists of two lobes capping opposite poles. For x-polarised illumination, both lobes extend into the dye, whereas for z polarisation, one lobe extends into the nonfluorescent fiber tip.

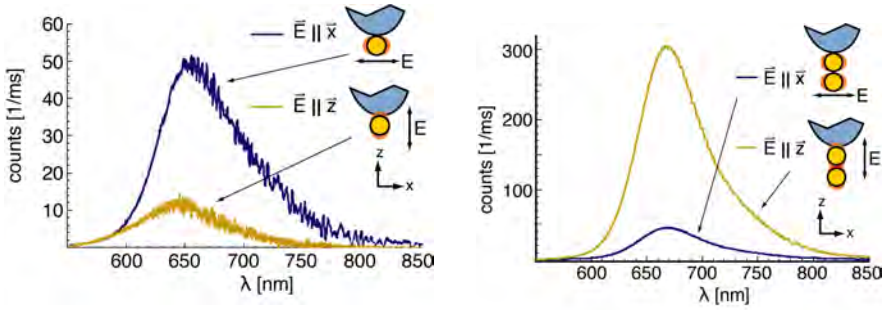

Fig. 10. Fluorescent spectra of Nile Blue for two focal polarisations. *Left* A single Au 80 nm sphere. *Right*. Two Au 80 nm spheres, the second attached to the first.

In a second step, a second Au sphere of 80 nm diameter is attached to the first one, as described in section 2.2.6. In a direct comparison, Fig.10 *right*, the fluorescence intensity is higher for both polarizations. While the signal for horizontal polarisation remained about the same, the signal for vertical polarisation increased enormously - this can be assigned to the enhanced near-field intensity between the two spheres.
A rotation check, i.e. rotating the fiber probe and the polarisation with respect to each other, provides an intensity variation of only 10%, Fig.11 hints that the two particles are close to the symmetric orientation V. in Fig.8.

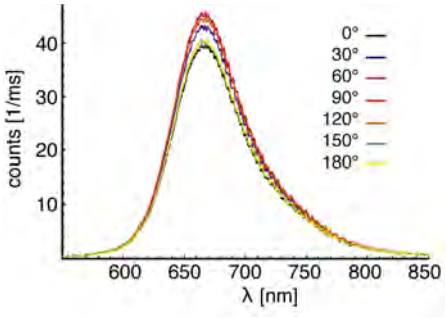

Fig. 11. Orientation-dependent fluorescence in the vicinity of two 80 nm Au spheres. The horizontal polarisation and the probe are rotated around the z-axis. The peak intensity varies by about 10%.

In a third step, the experiment is repeated with a 80 nm particle which carries a smaller particle of 30 nm diameter (both Au). A basic check with excitation light polarised along x,y,z, Fig.12 *left*, shows that the z-direction is not as pronounced anymore as in Fig.10 *right*. The rotation

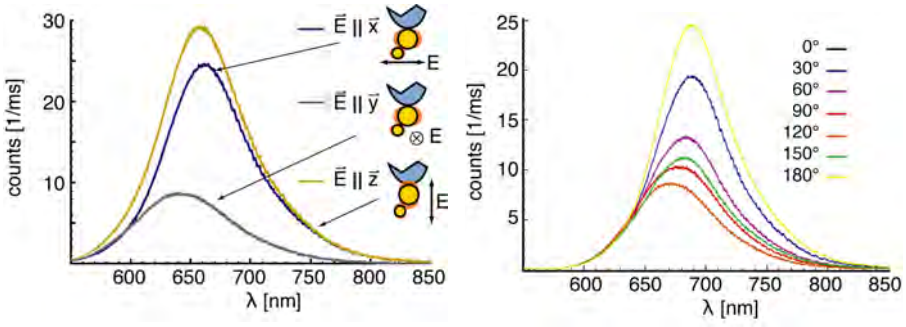

Fig. 12. Orientation-dependent fluorescence in the vicinity of a pair of 80 nm + 30 nm Au spheres. *Left*. The fluorescence intensity for x- and z-oriented excitation polarisation are rather similar, whereas in-plane y-polarisation provides a rather small signal. *Right* A rotational analysis reveals that the peak intensity varies by more than 50%.

check, Fig.12 *right*, shows a significant intensity variation for various relative orientations. This hints that the relative particle orientation is rather close to image VIII. in Fig.8, with the principal axis along x direction. In comparison to the two Au particles of equal size one realises that the principal axis here is not just slightly off the plumb line, but by a significant angle.

What’s more: considering the property of the scattering cross section, equation (1), a single 30 nm particle is supposed to be nearly irrelevant in comparison to a 80 nm sphere, as the volume squares V_{30}^2/V_{80}^2, and hence their scattering cross sections, C_{sc30}/C_{sc80}, have a ratio of less than 0.003. But thanks to near-field-mediated coupling of the two particles’ plasmons, the smaller particle has a significant impact on the fluorescence in the vicinity of the particle pair. So by combining particle-decorated probe tips with a straight-forward fluorescence analysis it is possible to learn a lot about the particles and their relative orientation. This is a valuable simplification of a lab workflow: For many applications, it is already sufficient to know the direction of the projected principal axis – the tedious procedure (of mounting the tip, attaching particles, unmounting the tip keeping its orientation in mind, moving it into an electron microscope, get the particle orientation, return the tip to the optical setup while maintaining the orientation according to the SEM coordinates) is dodged. Note that for these experiments, actual *distance-controlled scanning* of the probe tip was used only for the act of mounting the particles – the orientation determination took place well off the cover slide surface.

4. Conclusion & outlook

At this point, the principles of scanning particle microscopy were explained. The technical details and "tricks" were given, and the reader should be able to follow up according to her/his own experiments. Not to use the most pointed tips available, and to exploit the properties of immersion liquids may be valuable hints.

The Application section underlined the versatility of particle-decorated probes as mobile hot spots, *i.e.* as optical antennas providing locally enhanced intensities. As an example how well the third dimension can be explored by "pulling the strings", fluorescence in the vicinity of Au nanoparticle pairs was analysed.

The given procedures are not exhaustive, but a dexterous experimentalist, after checking

alternatives (Eng et al., 2010), may make use of the information here – the technology and its scientific applications are not maxed out yet, and many interesting experiments can be expected in the future.

5. Acknowledgements

The author wishes to thank Thomas Kalkbrenner for long-term inspiration on this topic, and Lukas M. Eng, Marc-Tobias Wenzel, and Thomas Härtling for providing a productive climate in the SNOM lab of the Institute for Applied Photophysics at the TU Dresden, Germany. Helge Weman of the Institute of Electronics and Telecommunications at the NTNU Trondheim, Norway, deserves gratitude for endorsing the writing of this scripture.

6. References

E. Abbe (1904). *Gesammelte Abhandlungen. Bd. 1: Theorie des Mikroskops.* G. Fischer, Jena.

M. S. Anderson (2000). Locally enhanced Raman spectroscopy with an atomic force microscope. *Appl. Phys. Lett.*, Vol. 76 no. 21, pp. 3130ff.

L. Aigouy, B. Samson, G. Julié, V. Mathet, N. Lequeux, C. N. Allen, H. Diaf, & B. Dubertret (2006). Scanning near-field optical microscope working with a CdSe/ ZnS quantum dot based optical detector. *Rev. Sci. Instrum.*, Vol. 77, 063702.

E. Bailo & V. Deckert (2008). Tip-enhanced Raman spectroscopy of single RNA strands: Towards a novel direct-sequencing Method. *Angew. Chemie Internat. Ed.*, Vol. 47, pp. 1658-1661.

G. Balasubramanian, I. Y. Chan, R. Kolesov, M. Al-Hmoud, J. Tisler, Chang Shin, Changdong Kim, A. Wojcik, P. R. Hemmer, A. Krueger, T. Hanke, A. Leitenstorfer, R. Bratschitsch, F. Jelezko, & J. Wrachtrup. Nanoscale imaging magnetometry with diamond spins under ambient conditions. *Nature*, Vol. 455, pp. 648-651.

A. Bek, R. Jansen, M. Ringler, S. Mayilo, T. A. Klar, & J. Feldmann (2008). Fluorescence enhancement in hot spots of AFM-designed gold nanoparticle sandwiches. *Nano Lett.* Vol. 8 no. 2, pp. 485-490.

P. Bharadwaj, P. Anger, & L. Novotny (2007). Nanoplasmonic enhancement of single-molecule fluorescence. *Nanotechnology*, Vol. 18, 044017.

D. Boyer, P. Tamarat, A. Maali, B. Lounis, & M. Orrit (2002). Photothermal imaging of nanometer-sized metal particles among scatterers. *Science* Vol. 297, pp. 1160-1163.

M. Brust, D. J. Schiffrin, D. Bethell, & C. J. Kiely (1995). Novel gold-dithiol nano-networks with non-metallic electronic properties. *Adv. Mater.*, Vol. 7 no. 9, pp. 795ff.

M. Danckwerts & L. Novotny. Optical frequency mixing at coupled gold nanoparticles. *Phys. Rev. Lett.*, Vol. 98, 026104.

R. C. Dunn (1999). Near-field scanning microsopy. *Chem. Rev.* Vol. 99 no. 10, pp. 2891-2927.

L. M. Eng, T. Härtling, & P. Olk (2010). Device and method for metallizing scanning probe tips. *Int. patent application*, PCT/DE2010/000579.

M. Fleischer, C. Stanciu, F. Stade, J. Stadler, K. Braun, A. Heeren, M. Häffner, D. P. Kern, & A. J. Meixner. Three-dimensional optical antennas: Nanocones in an apertureless scanning near-field microscope. *Appl. Phys. Lett.*, Vol. 93 no. 11, 111114.

H. G. Frey, S. Witt, K. Felderer, & R. Guckenberger (2004). High-resolution imaging of single fluorescent molecules with the optical near-field of a metal tip. *Phys. Rev. Lett.*, Vol. 93, 200801.

T. Härtling, Y. Alaverdyan, M. T. Wenzel, R. Kullock, M. Käll, & L. M. Eng (2008). Photochemical tuning of plasmon resonances in single gold nanoparticles. *J. Phys. Chem. C*, Vol. 112 no. 13, pp. 4920-4924.

T. Härtling, T. Uhlig, A. Seidenstücker, N. C. Bigall, P. Olk, U. Wiedwald, L. Han, A. Eychmüller, A. Plettl, P. Ziemann, & L. M. Eng (2010). Fabrication of two-dimensional Au@FePt core-shell nanoparticle arrays by photochemical metal deposition. *Appl. Phys. Lett.*, Vol. 96, 183111.

M. J. Howes & D. V. Morgan (1980). *Optical Fiber Communications - Devices, Circuits, and Systems*, John Wiley & Sons Ltd., ISBN 0-471-27611-1.

J. Jiang, K. Bosnick, M. Maillard, & L. Brus (2003) Single molecule Raman spectroscopy at the junctions of large Ag nanocrystals. *J. Phys. Chem. B*, Vol. 107 no. 37, pp. 9964-9972.

J. C. Johnson, H. Yan, R. D. Schaller, L. H. Haber, R. J. Saykally, & P. Yang (2001). Single nanowire lasers. *J. Phys. Chem. B*, Vol. 105 no. 46, pp. 11387-11390.

T. Kalkbrenner, M. Ramstein, J. Mlynek, & V. Sandoghdar (2001). A single gold particle as a probe for apertureless scanning near-field optical microscopy. *J. Microscopy* Vol. 202, pp. 72-76.

T. Kalkbrenner, U. Håkanson, & V. Sandoghdar (2004). Tomographic plasmon spectroscopy of a single gold nanoparticle. *Nano Lett.* Vol. 4 no. 12, pp. 2309-2314.

S. C. Kehr, M. Cebula, O. Mieth, T. Härtling, J. Seidel, S. Grafström, L. M. Eng, S. Winnerl, D. Stehr, & M. Helm. Anisotropy contrast in phonon-enhanced apertureless near-field microscopy using a free-electron laser. *Phys. Rev. Lett.* Vol. 100 no. 25, 256403.

K. Li, M. I. Stockman, & D. J. Bergman (2003). Self-similar chain of metal nanospheres as an efficient nanolens. *Phys. Rev. Lett.*, Vol. 91, 227402.

S. Nie & S. R. Emory (1997). Probing single molecules and single nanoparticles by surface-enhanced Raman scattering. *Science*, Vol. 275 no. 5303, pp. 1102-1106.

P. Olk, J. Renger, T. Härtling, M. T. Wenzel, & L. M. Eng (2007). Two particle enhanced nano Raman microscopy and spectroscopy. *Nano Lett.*, Vol. 7, no. 6, pp. 1736-1740.

P. Olk, J. Renger, M. T. Wenzel, & L. M. Eng (2008). Distance dependent spectral tuning of two coupled metal nanoparticles. *Nano Lett.*, Vol. 8 no. 4, pp. 1174-1178.

P. Olk (2008). *Optical Properties of Individual Nano-Sized Gold Particle Pairs*. Dissertation, TU Dresden, *http://nbn-resolving.de/urn:nbn:de:bsz:14-ds-1218612352686-00553*.

P. Olk, T. Härtling, R. Kullock, & L. M. Eng (2010). Three-dimensional, arbitrary orientation of focal polarization. *Appl. Optics*, Vol. 49 no. 23, pp. 4479-4482.

P. Pramod & K. G. Thomas (2008). Plasmon coupling in dimers of Au nanorods. *Adv. Mater.* Vol. 20 no. 22, pp. 4300-4305.

T. G. Philbin, C.Kuklewicz, S. Robertson, S. Hill, F. König, & U. Leonhardt (2008). Fiber-optical analog of the Event Horizon. *Science*, Vol. 319 no. 5868, pp. 1367-1370.

W. Plieth, H. Dietz, G. Sandmann, A. Meixner, M. Weber, P. Moyer, & J. Schmidt (1999). Nanocrystalline structures of metal deposits studied by locally resolved Raman microscopy. *Electrochimica Acta*, Vol. 44 no. 21-22, pp. 3659-3666.

W. Rechberger, A. Hohenau, A. Leitner, J. R. Krenn, B. Lamprecht, & F. R. Aussenegg (2003). Optical properties of two interacting gold nanoparticles. *Opt. Comm.* Vol. 220 no. 1-3, pp. 137-141.

V. Sandoghdar & J. Mlynek (1999). Prospects of apertureless SNOM with active probes. *J. Opt. A: Pure and Appl. Opt.* Vol. 1 no. 4, pp. 523-530.

C. Sönnichsen (2001). *Plasmons in Metal Nanostructures.* Cuviller, Göttingen.

N. Stephenson (1996). Mother Earth Mother Board. *Wired*, Vol. 12, ISSN 1059-1028.

R. Stöckle, Y. D. Suh, V. Deckert, & R. Zenobi (2000). Nanoscale chemical analysis by tip-enhanced Raman scattering. *Chem. Phys. Lett.* Vol. 318, pp. 131 - 136.

E. Udd (1990). *Fiber Optic Sensors*, Wiley Interscience, ISBN 0-471-83007-0.

B. Uhlig, J.-H. Zollondz, M. Haberjahn, H. Bloeß, & P. Kücher (2007). Nano-Raman: Monitoring nanoscale stress. *AIP Conf. Proc.*, Vol. 931 pp. 84-88.

M. T. Wenzel, T. Härtling, P. Olk, S. C. Kehr, S. Grafström, S. Winnerl, M. Helm, & L. M. Eng (2008). Gold nanoparticle tips for optical field confinement in infrared scattering near-field optical microscopy. *Opt. Express*, Vol. 16, pp. 12302-12312.

J. Wessel (1985). Surface-enhanced optical microscopy. *J. Opt. Soc. Am. B*, Vol .2 no. 9, pp. 1538-1541.

F. Zolla, G. Renversez, A. Nicolet, B. Kuhlmey, S. Guenneau, & D. Felbacq (2005). *Foundations Of Photonic Crystal Fibers*, Imperial College Press, ISBN 1-86094-507-4.